

Non-equilibrium Green's function approach to low-energy fission dynamics

K. Uzawa,¹ K. Hagino,¹ and G.F. Bertsch²

¹ *Department of Physics, Kyoto University, Kyoto 606-8502, Japan*

² *Department of Physics and Institute for Nuclear Theory, Box 351560, University of Washington, Seattle, Washington 98195, USA*

The concept of a compound nucleus was proposed by Bohr in 1936 to explain narrow resonances in neutron scattering off a nucleus. While a compound nucleus has been understood in terms of statistical mechanics, its description based on a many-body Hamiltonian has yet to be developed. Here we present a microscopic modeling of a compound nucleus starting from a nucleonic degree of freedom. We focus in particular on a decay of a heavy compound nucleus, that is, fission and radiative capture. To this end, we develop an approach based on a non-equilibrium Green's function, which is combined with a configuration interaction (CI) approach based on a constrained density-functional theory (DFT). We apply this approach to a barrier-top fission of ^{236}U , restricting the model space to seniority zero configurations of neutrons and protons. Our calculation with a Skyrme energy functional yields the fission-to-capture branching ratio of around 0.07. While this value is still reasonable, the calculation underestimates the branching ratio by about a factor of 40 as compared to the empirical value, indicating a necessity of seniority non-zero configurations in the model space. We also find that the distribution of the fission probability approximately follows the chi-squared distribution with the number of degrees of freedom of the order of 1, which is consistent with the experimental finding.

Many narrow resonance peaks have been observed in total cross sections of a neutron scattering off a nucleus. To explain this, Niels Bohr proposed the concept of a compound nucleus [1]. That is, when a slow neutron is absorbed by a nucleus, the neutron collides many times with other nucleons inside the nucleus and loses its energy. The resultant nucleus, referred to as a compound nucleus, is in a thermal equilibrium and meta-stable having a small decay width. The concept of a compound nucleus has been one of the most important landmarks in nuclear physics.

A compound nucleus decays by emitting particles such as neutrons, protons, and alpha particles, or gamma rays. Heavy compound nuclei also decay via fission. In syntheses of superheavy nuclei, a severe competition between neutron evaporations and fission of a compound nucleus actually plays a crucial role [3]. It has been a custom to describe such decays of a compound nucleus using a statistical model [2, 4]. While a level density is an important microscopic input to a statistical model, dynamical calculations based on a many-body Hamiltonian has been rather scarce [5].

The purpose of this paper is to develop a microscopic description of decays of a heavy compound nucleus, particularly a competition between radiative capture and fission. There are many motivations for this. Firstly, in r-process nucleosynthesis, heavy neutron-rich nuclei may decay via fission, leading to a fission recycling [6–8]. Such heavy neutron-rich nuclei are located outside the experimentally known region, and a description of fission with a microscopic framework is desirable. Secondly, a neutron separation energy of neutron-rich nuclei is so small that a compound nucleus formed in r-process nucleosynthesis will be at relatively low excitation energies. One may then question the validity of a statistical model, and thus a microscopic approach would be more suitable in that

situation. This would be the case also for a barrier-top fission of stable nuclei, in which the excitation energy at a saddle of fission barrier will be small due to the presence of a barrier. An advantage of our model is that a competition between (n, γ) and (n, f) processes can be described within the same framework. Thirdly, because of a rapid increase of computer powers, a large scale calculation can now be performed much more easily than before. A microscopic description of fission has been an ultimate goal of nuclear physics, and we are now at the stage to tackle it with large scale calculations [5].

In this paper, we propose a novel microscopic approach to low-energy induced fission based on a configuration interaction (CI) method. For this purpose, we apply a non-equilibrium Green's function (NEGF) [9] to describe decay dynamics. This approach has been widely utilized to calculate a current and a charge density for problems of electron transport in nano-devices [10, 11]. A problem of fission has an analogous feature to this problem, as one has to estimate a transmission coefficient for a transition from a compound nucleus configuration to a pre-fission configuration. This can be viewed as a non-equilibrium current.

A preliminary calculation with this approach has been published in Ref. [12]. In that paper, the model space was reduced by considering only neutron seniority-zero configurations in ^{236}U . Moreover, only the dynamics around the first fission barrier was discussed while ^{236}U is known to have a double humped fission barrier. In this paper, we shall substantially enlarge the model space, including both neutrons and protons, and also both the first and the second fission barriers. Such extension of the model space allows a more consistent comparison with experimental data.

To describe the fission dynamics of ^{236}U , we first assume that fission takes place along a path characterized

by the mass quadrupole moment, Q_{20} . We further assume that the axial symmetry is retained during fission. To construct many-body configurations along the fission path, we discretize the path as $\{Q_k; k = 1, 2, \dots, N\}$ and obtain the local ground state at each quadrupole moment Q_k using the constrained density functional theory (DFT), in which a given energy functional is minimized with respect to the density under the condition that the expectation value of quadrupole moment coincides with Q_k . Each local ground state generates a deformation-dependent mean-field with deformation-dependent single-particle levels in it. We construct many-particle-many-hole configurations at each deformation, $\{|i, Q_k\rangle\}$, based on the single-particle levels at a given deformation. We call a set of $\{|i, Q_k\rangle\}$ for a fixed Q_k a Q -block. Those configurations are coupled to each other due to residual interactions: this is both within the same deformation and with different deformations. The resultant Hamiltonian matrix reads $H_{ik,jk'} = \langle i, Q_k | H | j, Q_{k'} \rangle$. Those configurations are in general not orthogonal to each other (except for those within the same Q_k), and one also needs to compute the overlap matrix, $\mathcal{N}_{ik,jk'} = \langle i, Q_k | j, Q_{k'} \rangle$.

To treat a probability current, we introduce imaginary matrices, $-i\Gamma_a/2$, to the Hamiltonian matrix, where Γ_a corresponds to a decay width of a channel a to the space outside the model space explicitly considered in the Hamiltonian. In our problem, we consider decays of a compound nucleus via a neutron emission, gamma-ray emissions, and fission. Notice that the neutron emission is an inverse process of neutron absorption, and we refer to it as an incoming channel. We assume that the neutron emission and the gamma-ray emission takes place only from configurations with the smallest Q while the fission decay takes place only from configurations with the largest Q . The elements of the decay matrices then read,

$$(\Gamma_{\text{in}})_{ik,i'k'} = \gamma_{\text{in}} \delta_{i, \text{in}} \delta_{i', \text{in}} \delta_{k,1} \delta_{k',1}, \quad (1)$$

$$(\Gamma_{\text{cap}})_{ik,i'k'} = \gamma_{\text{cap}} \delta_{i,i'} \delta_{k,1} \delta_{k',1}, \quad (2)$$

$$(\Gamma_{\text{fis}})_{ik,i'k'} = \gamma_{\text{fis}} \delta_{i,i'} \delta_{k,N} \delta_{k',N}, \quad (3)$$

where $i = \text{in}$ is a single entrance channel. For simplicity, we have assumed that those decay matrices are diagonal. The transmission coefficient from a channel a to a channel b is computed with the Datta formula [10],

$$T_{a,b} = \text{Tr} [\Gamma_a G(E) \Gamma_b G^\dagger(E)], \quad (4)$$

where E is the excitation energy of a compound nucleus and $G(E)$ is the non-equilibrium Green's function given by

$$G(E) = \left(H - \frac{i}{2} \sum_a \Gamma_a - EN \right)^{-1}. \quad (5)$$

Let us apply the formalism to a neutron-induced fission reaction of ^{236}U , that is, $^{235}\text{U}(n, f)$, and numerically evaluate the transmission coefficients. We use **Skyax** [13] for a

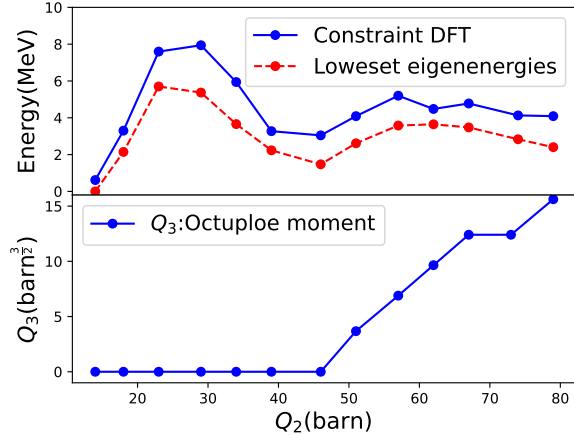


FIG. 1: (The upper panel) The fission barrier of ^{236}U along the fission path defined by the mass quadrupole moment, Q_2 . The blue solid line shows the energies of the local ground states obtained with the constrained DFT calculation. It is scaled by a factor of 0.71. The red dashed line shows the lowest eigenvalues obtained by diagonalizing each Q -block after scaling the blue solid line. The origin of the energy is set at the lowest eigenvalue at $Q_2 = 14$ b. (The lower panel) The octupole moment Q_3 in ^{236}U along the fission path.

DFT solver, in which the Kohn-Sham equation is solved in the cylindrical coordinate space. We use a Skyrme functional with the UNEDF1 parameter set [14], which has an effective mass close to unity and is thus suitable to reproduce a reasonable level density of excited nuclei. In constructing many-body configurations, we do not include the pairing interaction, which is however included later as a residual interaction.

The fission path is discretized with a criterion that the overlap of the local ground states between the nearest neighbors is $\mathcal{N} \sim e^{-1}$ [12, 15]. We extend the maximum value of Q up to around 80 b so that both the first and the second fission barriers are covered. The criterion for the discretization leads to 13 blocks from $Q = 14$ b to $Q = 79$ b. The potential energy curve for fission of ^{236}U is shown in the upper panel of Fig. 1 by the solid line as a function of the quadrupole moment Q_2 , together with the octupole moment Q_3 shown in the lower panel. In this calculation, the ground state is located at $Q_2 = 14$ b. There are two fission barriers, the first fission barrier around $Q_2 = 30$ b and the second barrier around $Q_2 = 60$ b. The fission path is along the mass symmetric path up to the first barrier, and it extends to the mass asymmetric path going through the second barrier, as is indicated in the lower panel of Fig. 1.

In the previous work [12], the many-body configurations were constructed solely with neutron excitations up to 4 MeV. In contrast, in this paper we extend the model space and take both neutron and proton excitations up to 5 MeV. Following Ref. [12], we shall take into account only seniority-zero configurations, that is, those without

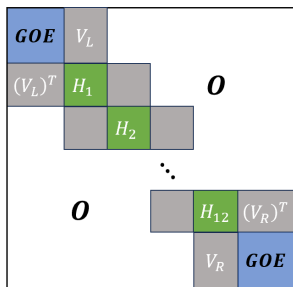


FIG. 2: A schematic illustration of the Hamiltonian matrix.

broken pairs. This permits collective dynamics but not diffusive dynamics [16] as the main mechanism for barrier crossing. The dimension of each Q -block is summarized in Table I.

For residual interactions, we take a monopole pairing interaction [12] as well as a diabatic interaction [17], the latter of which acts only between the diabatically connected configurations. For the strengths of these residual interactions, we take $G_{\text{pair}} = 0.16$ MeV and $h_2 = 1.5$ MeV for the pairing and the diabatic interactions, respectively. The value of G_{pair} is determined to reproduce the excitation energy of the first excited 0^+ state of ^{236}U within the model space so specified [12], while the value of h_2 is the same as the one used in Ref. [12].

The dashed line in the upper panel of Fig. 1 shows the potential energy curve connecting the lowest eigenvalue for each Q -block. To reproduce the experimentally determined barrier height of 5.7 MeV [18], we have introduced a multiplicative factor of 0.71 to the solid line and then diagonalized the Hamiltonian for each Q -block. The overestimation of the barrier may be attributed to the absence of the triaxial deformation [19].

As the dimension is still large for the Q -block at $Q_2 = 14$ b as well as the Q -block right after $Q_2 = 79$ b, we follow the previous calculation [12] and replace those with a random matrices sampled from the Gaussian Orthogonal Ensemble (GOE). We set the central energy of the matrices to be the same as the excitation energy, E . In addition to the central energy, the GOE is characterized by the root-mean-square of the matrix elements $\langle v^2 \rangle^{1/2}$ and the matrix dimension N_{GOE} . These parameters are related with the level density at the center of the distribution, $\rho_0 = N_{\text{GOE}}^{1/2} / \pi \langle v^2 \rangle^{1/2}$ [20]. In our calculations, we set $\rho_0 = 31.8$ MeV $^{-1}$ [12] and $N_{\text{GOE}} = 1000$.

Neglecting the couplings between the next-to-the-nearest neighboring Q -blocks, the structure of the resultant Hamiltonian matrix is schematically illustrated in Fig. 2. Here, H_i represents the matrix elements for the configurations at specific Q_i shown in Table I. The overlap matrix \mathcal{N} has a similar structure. With this simplification, the matrix $(H - E\mathcal{N})$ becomes block tri-diagonal, and its inverse can be efficiently calculated with the method presented in Ref. [21].

The last components of the Hamiltonian are the matrix elements of V_L and V_R connecting the ending Q -blocks to

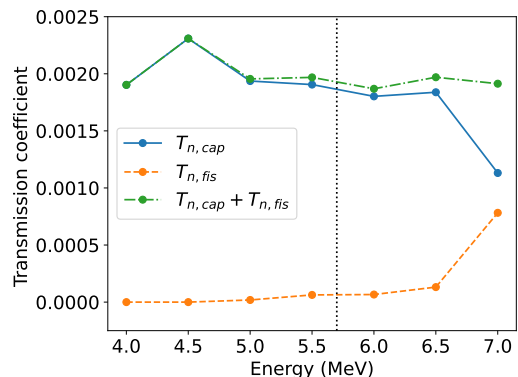


FIG. 3: The averaged transmission coefficients for capture $\langle T_{\text{in,cap}}(E) \rangle$ (the blue solid line) and for fission $\langle T_{\text{in,fis}}(E) \rangle$ (the orange dashed line) as a function of the excitation energy E . The sum of these transmission coefficients is also plotted with the green dot-dashed line. The vertical dotted line shows the height of the fission barrier located at 5.7 MeV.

the states in the GOEs. We assume that they also follow a Gaussian distribution, with root-mean-square strengths of $\sqrt{\langle v_a^2 \rangle} = 0.02$ MeV and $\sqrt{\langle v_b^2 \rangle} = 0.03$ MeV, respectively. Those order of magnitude may be justified as follows. The present calculation with the UNEDF1 parameter set yields the level density of $\rho_{\text{tot}} = 3.87 \times 10^5$ MeV $^{-1}$ for $K^\pi = 0^+$ configurations, where K is the spin projection onto the symmetry axis, at the excitation energy $E = 6.5$ MeV. On the other hand, if the configurations are restricted only to the seniority zero, the level density is $\rho_{\nu=0} = 220$ MeV $^{-1}$ at the same excitation energy. If one scales the strength of the diabatic interaction according to the level densities, the strength of a residual interaction is estimated to be $v = h_2 \sqrt{\rho_{\nu=0} / \rho_{\text{tot}}} \sim 0.036$ MeV for $h_2 = 1.5$ MeV. This is close to the values of v_a and v_b which we employ.

Let us now numerically evaluate the transmission coefficients, $T_{\text{in,cap}}$ and $T_{\text{in,fis}}$. To this end, following the Appendix in Ref. [12], we set $\gamma_{\text{in}} = 0.01$ MeV and $\gamma_{\text{cap}} = 0.00125$ MeV, respectively. For γ_{fis} , we arbitrarily set it to be 0.015 MeV, as it has been found that transmission coefficients are insensitive to the value of γ_{fis} [12, 22]. Experimentally, decay widths are measured within an energy resolution. We thus introduce an energy average,

$$\langle T_{\text{in},a}(E) \rangle = \frac{1}{\Delta E} \int_{E-\Delta E/2}^{E+\Delta E/2} dE' T_{\text{in},a}(E'), \quad (6)$$

where ΔE is an energy interval. We take $\Delta E = 0.25$ MeV, which satisfies the condition $\Delta E \gg 1/\rho_0$. Furthermore, we take an ensemble average with 100 samples of the transmission coefficients. Fig. 3 shows the energy dependence of the transmission coefficients so obtained for the capture (the solid line) and the fission (the dashed line). $\langle T_{\text{in,fis}}(E) \rangle$ increases as the excitation energy increases, while $\langle T_{\text{in,cap}}(E) \rangle$ decreases be-

Q_2 (barn)	18	23	29	34	39	46	51	57	62	67	74	79
dim.	2520	9794	15088	11577	2774	2940	3021	3150	2196	3752	2871	4420

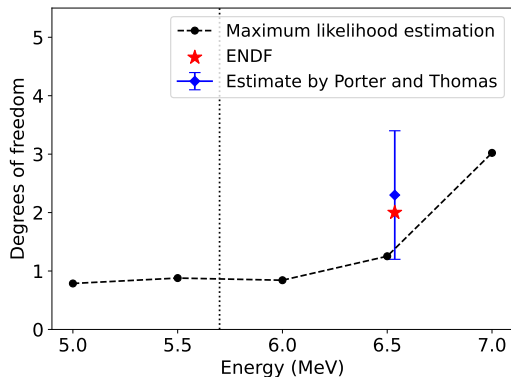
TABLE I: The dimension of each Q -block for fission of ^{236}U .

FIG. 4: The number of degrees of the freedom ν obtained by fitting the distribution of transmission coefficients for fission to the chi-squared distribution. The blue diamond is the empirical estimate of ν in Ref. [27], while the star represents the data from ENDF/B-VIII.0 [28, 29]. The vertical dotted line denotes the height of the fission barrier.

cause the total reaction probability is approximately conserved (see the dot-dashed line). At $E = 6.5$ MeV, which is close to the neutron separation energy of ^{236}U ($S_n = 6.536$ MeV) [23], the fission-to-capture branching ratio, $\alpha^{-1} \equiv \langle T_{\text{in, fis}} \rangle / \langle T_{\text{in, cap}} \rangle$, is 0.071 in this calculation. Even though this value is still reasonable, it underestimates the empirical value, $\alpha^{-1} \simeq 3$ [24], by a factor of about 40. One could increase the values of v_a and v_b to obtain a more reasonable branching ratio. However, we have found that the fluctuation of $T_{\text{in, fis}}(E)$ then largely deviates from the chi-squared distribution, which is inconsistent with experimental findings. Since we employ the justifiable values of v_a and v_b , this clearly indicates that one needs to further increase the model space to reproduce the empirical branching ratio. In fact, it would be expected that the agreement with the experimental branching ratio is improved by including seniority non-zero configurations and a proton-neutron random interaction which acts on that space [22, 25].

Another important quantity for induced fission is the number of degree of freedom, which is related to the effective number of decay channels. In order to study this, we examine a fluctuation of the fission probability defined by $P_{\text{fis}} \equiv T_{\text{in, fis}} / (T_{\text{in, fis}} + T_{\text{in, cap}})$ [26]. To this end, we fit the distribution of P_{fis} generated with 1000 samples for a specific excitation energy E with the chi-squared function defined by

$$P_\nu(x) = \frac{\nu}{2\Gamma(\nu/2)} \left(\frac{\nu x}{2}\right)^{\nu/2-1} e^{-\nu x/2}. \quad (7)$$

Here, the parameter ν is referred to as the number of degrees of freedom and Γ is the Gamma function. Fig.4 shows the energy dependence of the extracted ν . It is remarkable that the extracted ν is much smaller than the number of fission channels, that is, $N_{\text{GOE}} = 1000$ in this calculation. This is consistent with the picture of transition state theory [30–37], and our model yields it naturally even though we do not introduce a priori any assumption used in it [38]. We mention that the calculation somewhat underestimates the experimental data at $E = 6.5$ MeV, but this may be resolved by including seniority non-zero configurations as in the discussion on the branching ratio.

In summary, we presented a novel approach to low-energy induced fission based on the method of non-equilibrium Green’s function (NEGF), which has been widely used in problems of electron transport in condensed matter physics. To this end, we considered a model which consists of many-body configurations constructed with the constrained density functional theory. Compound nucleus configurations as well as pre-fission configurations were represented by random matrices. Transmission coefficients were then evaluated with the Datta formula in the NEGF formalism. We applied this method to neutron induced fission of ^{235}U by restricting to seniority-zero configurations. We found that the fission-to-capture branching ratio was somewhat underestimated, even though the calculated value was still reasonable. As we chose the parameters as realistic as possible, this clearly indicated a necessity of seniority non-zero configurations. We also evaluated the number of degrees of freedom ν for fission. Our calculation yielded much smaller values for ν as compared to the number of the fission decay channels, which is consistent with the experimental data as well as the picture of transition state theory.

The method presented in this paper provides a promising way to microscopically understand nuclear fission. A big challenge is how to manage the dimension of Hamiltonian matrix, which increases rapidly as the model space increases. In this connection, we plan to discuss in detail a fluctuation of decay widths and the number of degrees of freedom in a separate publication [39].

We thank D.A. Brown for useful discussions. This work was supported in part by JSPS KAKENHI Grants No. JP19K03861 and JP23K03414, and JP23KJ1212. The numerical calculations were performed with the computer facility at the Yukawa Institute for Theoretical Physics, Kyoto University.

-
- [1] N. Bohr, *Nature* **137**, 351 (1936).
- [2] P. Fröbrich and R. Lipperheide, *Theory of Nuclear Reactions* (Oxford Science Publications/Clarendon Press, Oxford, 1996).
- [3] S. Hofmann and G. Münzenberg, *Rev. Mod. Phys.* **72**, 733 (2000).
- [4] L. Hongliang, M. Anthony, Y. Abe, and D. Boilley, *Comp. Phys. Comm.* **200**, 381 (2016).
- [5] M. Bender, R. Bernard, G. Bertsch, S. Chiba, J. Dobaczewski, N. Dubray, S. Giuliani, K. Hagino, D. Lacroix, Z. Li, P. Magierski, J. Maruhn, W. Nazarewicz, J. Pei, S. Peru, N. Pillet, J. Randrup, D. Regnier, P.-G. Reinhard, L. Robledo, W. Ryssens, J. Sadhukhan, G. Scamps, N. Schunck, C. Simenel, J. Skalski, I. Stetcu, P. Stevenson, S. Umar, M. Verriere, D. Vretnar, M. Warda, and S. Aberg, *J. of Phys.* **G47**, 113002 (2020).
- [6] J.J. Cowan, C. Sneden, J.E. Lawler, A. Aprahamian, M. Wiescher, K. Langanke, G. Martínez-Pinedo, and F.-K. Thielemann, *Rev. Mod. Phys.* **93**, 015002 (2021).
- [7] M. Eichler, A. Arcones, A. Kelic, O. Korobkin, K. Langanke, T. Marketin, G. Martínez-Pinedo, I. Panov, T. Rauscher, S. Rosswog, C. Winteler, N. T. Zinner, and F.-K. Thielemann, *Astrophys. J.* **808**, 30 (2015).
- [8] S. Goriely, J.L. Sida, J.F. Lemaître, S. Panebianco, N. Dubray, S. Hilaire, A. Bauswein, and H.T. Janka, *Phys. Rev. Lett.* **111**, 242502 (2013).
- [9] K.Y. Camsari, S. Chowdhury, and S. Datta, in *Springer Handbook of Semiconductor Devices*, edited by M. Rudan, R. Brunetti, and S. Reggiani (Springer International Publishing, Cham, 2023), p. 1583.
- [10] S. Datta, *Electronic Transport in Mesoscopic Systems* (Cambridge University Press, Cambridge, 1995).
- [11] S. Datta, *Quantum Transport: Atom to Transistor* (Cambridge University Press, Cambridge, 2005).
- [12] G.F. Bertsch and K. Hagino, *Phys. Rev.* **C107**, 044615 (2023).
- [13] P.-G. Reinhard, B. Schuetrumpf, and J.A. Maruhn, *Comp. Phys. Comm.* **258**, 107603 (2021).
- [14] M. Kortelainen, J. McDonnell, W. Nazarewicz, P.-G. Reinhard, J. Sarich, N. Schunck, M. V. Stoitsov, and S. M. Wild, *Phys. Rev.* **C85**, 024304 (2012).
- [15] G.F. Bertsch and K. Hagino, *Phys. Rev.* **C105**, 034618 (2022).
- [16] P. Hänggi, P. Peter, and M. Borkovec, *Rev. Mod. Phys.* **62**, 251 (1990).
- [17] K. Hagino and G.F. Bertsch, *Phys. Rev.* **C105**, 034323 (2022).
- [18] L.J. Lindgren, A. Alm, and A. Sandell, *Nucl. Phys.* **A298**, 43 (1978).
- [19] A. Staszczak, A. Baran, J. Dobaczewski, and W. Nazarewicz, *Phys. Rev.* **C80**, 014309 (2009).
- [20] H.A. Weidenmüller and G.E. Mitchell, *Rev. Mod. Phys.* **81**, 539 (2009).
- [21] D.E. Petersen, H.H. B. Sørensen, P.C. Hansen, S. Skelboe, and K. Stokbro, *J. Comput. Phys.* **227**, 3174 (2008).
- [22] K. Uzawa and K. Hagino, *Phys. Rev.* **C108**, 024319 (2023).
- [23] L.C. Leal, H. Derrien, N.M. Larson, and R.Q. Wright, *Nucl. Sci. Eng.* **131**, 230 (1999).
- [24] M.S. Moore, J.D. Moses, G.A. Keyworth, J.W.T. Dabbs, and N.W. Hill, *Phys. Rev.* **C18**, 1328 (1978).
- [25] B.W. Bush, G.F. Bertsch, and B.A. Brown, *Phys. Rev.* **C45**, 1709 (1992).
- [26] K. Hagino and G.F. Bertsch, *Phys. Rev.* **E104**, L052104 (2021).
- [27] C.E. Porter and R.G. Thomas, *Phys. Rev.* **104**, 483 (1956).
- [28] D.A. Brown et al., *Nuclear Data Sheets* **148**, 1 (2018).
- [29] D.A. Brown, private communications.
- [30] N. Bohr and J.A. Wheeler, *Phys. Rev.* **56**, 426 (1939).
- [31] D.G. Truhalar, B.C. Garrett, and S.J. Klippenstein, *J. Phys. Chem.* **100**, 12771 (1996).
- [32] D.G. Truhalar, W.L. Hase and J.T. Hynes, *J. Phys. Chem.* **87**, 2664 (1983).
- [33] G. Mills and H. Jónsson, *Phys. Rev. Lett.* **72**, 1124 (1994).
- [34] W.H. Miller, *J. Chem. Phys.* **61**, 1823 (1974).
- [35] K.J. Laidler and M.C. King, *J. Phys. Chem.* **87**, 2657 (1983).
- [36] R.A. Marcus and O.K. Rice, *J. Phys. and Colloid Chem.* **55**, 894 (1951).
- [37] R.A. Marcus, *J. Chem. Phys.* **20**, 359 (1952).
- [38] G.F. Bertsch and K. Hagino, *J. Phys. Soc. Jpn.* **90**, 114005 (2021).
- [39] K. Uzawa, K. Hagino, and G.F. Bertsch, in preparation.